Soil Biology & Biochemistry 50 (2012) 66–76

Contents lists available at SciVerse ScienceDirect

Soil Biology & Biochemistry

journal homepage: www.elsevier.com/locate/soilbio

Analytical models of soil and litter decomposition: Solutions for mass loss and time-dependent decay rates

Stefano Manzoni [a,b,*], Gervasio Piñeiro [b,c], Robert B. Jackson [b,d], Esteban G. Jobbágy [e], John H. Kim [d], Amilcare Porporato [a,b]

[a] Civil and Environmental Engineering Dept., Box 90287, Duke University, Durham, NC 27708-0287, USA
[b] Nicholas School of the Environment, Box 90328, Duke University, Durham, NC 27708, USA
[c] IFEVA/CONICET, Facultad de Agronomia, Universidad de Buenos Aires, Buenos Aires, Argentina
[d] Department of Biology, Box 90338, Duke University, Durham, NC 27708, USA
[e] Grupo de Estudios Ambientales, IMASL, Universidad Nacional de San Luis & CONICET, San Luis, Argentina

ARTICLE INFO

Article history:
Received 29 October 2011
Received in revised form
18 January 2012
Accepted 24 February 2012
Available online 23 March 2012

Keywords:
Soil organic matter and litter decomposition
Carbon model
Apparent decay rate
Linear systems
Compartment model
Continuous quality model

ABSTRACT

Combining decomposition data with process-based biogeochemical models is essential to quantify the turnover of organic carbon (C) in surface litter and soil organic matter (SOM). Long-term decomposition may be suitably analyzed by linear models (i.e., all fluxes defined by first-order kinetics), which allow the derivation of analytical expressions to estimate the loss of C and the overall apparent decay rate (k_{app}) through time. Here we compare eight linear models (four discrete-compartment models with one or two C pools, two models with a single time-dependent decay rate, and two models based on a continuous distribution of decay rates) and report their analytical solutions for two types of decomposition experiments: i) studies that evaluate the decomposition of a single input of fresh litter (i.e., a single cohort, as in litterbag and C labeling experiments), and ii) studies that evaluate the decomposition of soil samples with compounds of different ages (i.e., multiple cohorts, as in long-term incubations or isotope dilution experiments). We fitted analytical mass loss functions to both types of datasets and evaluated the performance of the models. For single-cohort data, continuous-decay models provide the best balance between accuracy and parsimony ($R^2 = 0.99$, lowest Akaike and Bayesian information criteria), while for multiple-cohort data the two-pool models tend to perform better ($R^2 = 0.96$), perhaps because of the strong separation of time scales in the decomposition data considered. Differences among some models are marginal, suggesting that decomposition data alone do not point to a single 'best' model. All models resulted in apparent decay rates that decreased markedly through time, in contrast with the assumption of constant k adopted in the single-pool exponential decay model. We also show how model parameters estimated from single cohort samples can be used to model multiple cohort decomposition, unifying both types of experimental data in one theory. Based on our results, it is possible to distinguish the temporal changes in C loss that are attributable to initial chemical composition or abiotic factors, from those associated with the presence of multiple ages in the substrate.

1. Introduction

Decomposition of organic matter is a biologically mediated biogeochemical process that controls ecosystem carbon (C) turnover and nutrient availability (Jenny et al., 1949; Jobbágy and Jackson, 2000; Berg and McClaugherty, 2003; Cebrian and Lartigue, 2004; Manzoni et al., 2010). The speed of microbial degradation depends on climatic conditions, as well as chemical recalcitrance and physical accessibility of C compounds. During decomposition, microbes transfer organic matter through compartments of different chemical quality, thereby altering the chemistry and physical accessibility of organic C. Conceptual models of decomposition are thus often based on networks of compartments accounting for the chemical heterogeneity of the original substrate and chemical and physical changes driven by microbial activity and environmental factors.

These compartment networks are the conceptual basis of most current biogeochemical models (Plante and Parton, 2007; Manzoni and Porporato, 2009). Each compartment is described by a mass

* Corresponding author. Civil and Environmental Engineering Dept., Box 90287, Duke University, Durham, NC 27708-0287, USA. Tel.: +1 919 6605467.
E-mail address: stefano.manzoni@duke.edu (S. Manzoni).

0038-0717/$ – see front matter © 2012 Elsevier Ltd. All rights reserved.
doi:10.1016/j.soilbio.2012.02.029

balance equation, and the connections represent fluxes of matter moving through the compartments. The fluxes can be described mathematically in different ways, but when the goal is to quantify long-term decomposition (i.e., annual or longer time scale) linear models are generally appropriate (Manzoni and Porporato, 2009). In a linear model, each pool is considered well-mixed and chemically homogeneous, and the decomposition rate is assumed to be controlled by the available substrate. The proportion of organic matter decomposed per unit time is therefore constant and equal to the decay (or kinetic) rate constant, k. Kinetic constants account for chemical and climatic conditions and thus vary across organic matter types and sites. Moreover, at these time scales, seasonal and higher-frequency climatic variability can be neglected, so that the decay constant for each compartment is effectively constant through time. Most biogeochemical models can thus be regarded as time-invariant linear networks, for which a well-developed theoretical basis exists (Eriksson, 1971; Feng, 2009a; Manzoni et al., 2009).

The main difficulties in this approach are the choice of the specific compartment network and the estimation of the decay rates. Several network structures have been proposed, ranging from simple one- or two-compartment models, to complex multi-compartment ones where serial, parallel, and feedback configurations coexist (Thuries et al., 2001; Pansu et al., 2004; Manzoni et al., 2009). Models that assume a distribution of decay rates have also been developed, on the grounds that chemical and physical heterogeneities are better described by a continuous distribution (heterogeneous pool) rather than by discrete compartments (homogeneous well-mixed pools) (Ågren and Bosatta, 1996; Bolker et al., 1998; Forney and Rothman, 2007; Feng, 2009b; Bruun et al., 2010; Sierra et al., 2011). The choice of the network depends on the goal of the model, with simpler models generally preferred for larger-scale, longer-term applications or where calibration datasets are limited. The values for the decay rates have been related to chemical, climatic, ecological, and edaphic factors (Parton et al., 1987, 2007; Aerts, 1997; Cebrian, 1999; Jobbágy and Jackson, 2000; Berg and McClaugherty, 2003; Cornwell et al., 2008; Zhang et al., 2008; Hui and Jackson, 2009), but also depend on model structure (Thuries et al., 2001; Pansu et al., 2004; Derrien and Amelung, 2011). To date, however, there is no consensus regarding either the choice of the biogeochemical network or the functional relationships between decay rates and environmental factors. It is thus important to explore systematically the patterns in decay rates for different model networks. One approach for achieving this goal is to fit the modeled C decay to observations from either litterbags or soil organic matter decomposition experiments (Wieder and Lang, 1982; Thuries et al., 2001; Parton et al., 2007; Zhang et al., 2007; Adair et al., 2008; Rovira and Rovira, 2010; Derrien and Amelung, 2011).

Our objectives here are to analyze eight commonly used biogeochemical models (both discrete compartment and continuous-quality models, see Table 1) and provide analytical solutions of organic matter C loss through time that can be used to estimate the decay rates from two typical decomposition datasets: i) litterbag studies and C labeling experiments, where one organic matter cohort is followed through time, and ii) SOM decomposition

Table 1
Overview of decomposition model structure and features. For each model, x_i indicates the C mass in i, k_i is the first-order decay rate, r and α are partitioning coefficients, and a, b, and m are shape factors.

Model	ID	Scheme	Mass balance equations	Mean transit time $\bar{\tau}$
One compartment	D1		$\frac{dx}{dt} = -kx$	$1/k$
Two compartments in series	D2	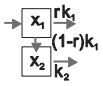	$\frac{dx_1}{dt} = I - k_1 x_1$ $\frac{dx_2}{dt} = (1-r)k_1 x_1 - k_2 x_2$	$\frac{(1-r)k_1 + k_2}{k_1 k_2}$
Two compartments in parallel	D3		$\frac{dx_1}{dt} = \alpha I - k_1 x_1$ $\frac{dx_2}{dt} = (1-\alpha) I - k_2 x_2$	$\frac{(1-\alpha)k_1 + \alpha k_2}{k_1 k_2}$
Feedback model	D4	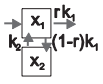	$\frac{dx_1}{dt} = I + k_2 x_2 - k_1 x_1$ $\frac{dx_2}{dt} = (1-r)k_1 x_1 - k_2 x_2$	$\frac{(1-r)k_1 + k_2}{r k_1 k_2}$
Feng and Li (2001)	L1[a]		$\frac{dx}{dt} = -\frac{a}{b}\left(\frac{t}{b}\right)^{a-1} x$	$b\Gamma\left(\frac{1}{a}+1\right)$
Rovira and Rovira (2010)	L2[b]		$\frac{dx}{dt} = -(a + be^{-mt})x$	$\frac{e^{-\frac{b}{m}}}{a}\,{}_1F_1\left(\frac{a}{m};\frac{a}{m}+1;\frac{b}{m}\right), a>0$
Gamma $p_k(k)$ (Bolker et al., 1998)	C1	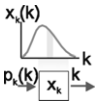	$\frac{dx}{dt} = -\int_0^\infty k x_k dk$ $p_k(k) = \frac{b^a}{\Gamma(a)} k^{a-1} e^{-bk}$	$\frac{b}{a-1}, \quad a>1$
Log-uniform $p_k(k)$ (Forney and Rothman, 2007)	C2		$\frac{dx}{dt} = -\int_0^\infty k x_k dk$ $p_k(k) = \frac{1}{\ln(b/a)k}, a \le k \le b$	$\frac{b-a}{ab\ln(b/a)}$

[a] $\Gamma(\cdot)$: gamma function.
[b] ${}_1F_1(\cdot;\cdot;\cdot)$: Kummer confluent hypergeometric function (Abramowitz and Stegun, 1972).

studies, where multiple cohorts (i.e., compounds of different age) decompose in the same sample. The analytical solutions obtained for these two decomposition experiments are first used to evaluate the performance of the models for both single cohort and multiple cohort studies. We then calculate the 'apparent' decay rate, denoted here as k_{app} (but also referred to as relative decomposition rate), i.e., the first-order decay rate for the total C in the system. Though the decay constants for each compartment are time-invariant, this apparent decay rate changes through time, depending upon model structure and type of decomposition study. Finally, by comparing mass loss and k_{app} in single- and multiple-cohort studies, we discuss how these results could be used to separate the drivers of decomposition in surface litter and mineral soils.

2. Methods

Soil and litter biogeochemical models are generally formulated through systems of ordinary differential equations, each representing the mass balance of an organic matter compartment (e.g., fresh litter, soluble C, microbial biomass, etc.). The system receives an input (litterfall or soil amendment), denoted by $I(t)$, which is redistributed among the compartments and lost through heterotrophic respiration and leaching (see Table 1 for the mass balance equations for each model considered). If the mass transfers among the compartments are defined by time-invariant first-order kinetics, the total mass of C in the system, $x(t)$, can be computed as (Eriksson, 1971; Manzoni et al., 2009)

$$x(t) = \int_0^\infty I(t-\tau)A(\tau)d\tau, \tag{1}$$

where $A(\tau)$ is the survivor function of the system, that is the proportion of C that remains in the soil or litter for at least a time τ. As a consequence, the mean transit (or residence) time is given by $\bar{\tau} = \int_0^\infty A(\tau)d\tau$. Eq. (1) essentially calculates the mass at any time t as the sum of the previous inputs $I(t-\tau)$, weighted by the probability $A(\tau)$ of remaining in the system for at least a time τ. Any time-invariant linear system can be recast in the form of Eq. (1), using the appropriate survivor function, which embeds all the information necessary to characterize the system, including structural properties such as the number of compartments and their connections and kinetic properties such as the values of the decay rates. Because of the properties of time-invariant linear systems, $A(\tau)$ can be obtained analytically as a function of the network structure. In fact, $A(\tau)$ is defined as the exceedance probability of the transit time distribution of the whole system, which in turn is determined by combining the transit time distributions of the individual pools of the network. This procedure is discussed in detail elsewhere (Manzoni et al., 2009). For the specific applications here, we build on this theory and apply it to decomposition experiments. The equations for survivor function and mean transit time reported in Tables 1 and A1 are employed as a starting point.

For any litterfall time series (represented by $I(t)$) and network structure (embedded in $A(t)$), the form of Eq. (1) allows the computation of mass loss, or $x(t)$, for any input function, including cases that are particularly relevant for interpreting decomposition datasets. Most litterbag experiments follow mass loss of fresh litter in a confined system that receives a single input (Fig. 1A). In this case all of the organic matter that is decomposed has the same age (i.e., a single cohort is being tracked). In contrast, soil organic matter decomposition follows the degradation of a mixture of compounds deposited to the soil at different times (Fig. 1B). In this case, the soil sample may be left to decompose without further input, or a rapid change in input rate can be imposed, for instance through a change in vegetation type or lab incubation. These two cases are treated separately below.

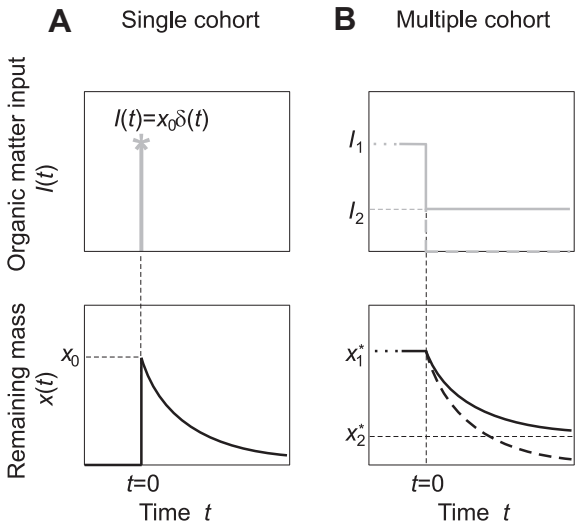

Fig. 1. Schematic representation of the time series of input, $I(t)$, and organic matter mass (or C), $x(t)$, in the two types of experiments considered. A) Single input of organic matter (with homogeneous age) at time $t = 0$ and subsequent mass loss (e.g., litterbag and pulse labeling experiments). B) Step change in input from I_1 to I_2 at $t = 0$ and subsequent change in organic matter mass from the equilibrium x_1^* to a new equilibrium x_2^* (in this example, the input decreases, resulting in decreased mass). The case $I_2 = 0$ (thick dashed curves in B) corresponds to decomposition of soil samples without amendments (lab incubations and bare fallow experiments); the case $I_2 > 0$ to changes in land use that alter productivity and hence organic matter inputs to the soil.

2.1. Single input (one cohort) studies: litterbag decomposition experiments

When a mass x_0 of organic matter is added once and left to decompose (as in the case of litterbags or a tracer pulse), the input to the system can be described by an instantaneous pulse, represented mathematically by a Dirac delta function, $I(t-\tau) = x_0\delta(t-\tau)$ (Fig. 1A). In this case, Eq. (1) can be solved to yield a relationship between the fraction of mass remaining and the survivor function,

$$\frac{x(t)}{x_0} = A(t) \tag{2}$$

Based on the time evolution of the organic matter mass, it is now possible to calculate the 'apparent' decay rate $k_{app}(t)$, that is the time-dependent first-order kinetic constant that can be used to describe any decomposition model through a single mass balance equation,

$$\frac{dx(t)}{dt} = -k_{app}(t)x(t), \tag{3}$$

with initial condition $x(0) = x_0$. Accordingly, $k_{app}(t)$ can be computed as a function of the survivor function as

$$k_{app}(t) = -\frac{dx(t)/dt}{x(t)} = -\frac{d\ \ln[A(t)]}{dt} \tag{4}$$

Note that the complexity of the original time-invariant system is now captured by a single time-dependent kinetic coefficient, $k_{app}(t)$. Because $k_{app}(t)$ depends on $x(t)$ and hence the history of the system, it may change in different decomposition experiments, as discussed below. Specific expressions of single-cohort $x(t)$ and $k_{app}(t)$ for each selected model are reported in Table A1.

2.2. Continuous inputs (multiple cohort) studies: SOM decomposition experiments

Unlike litterbags experiments, where all the organic matter is added at once, other types of experiments follow organic matter mass through time after a rapid change in input. For example, SOM (assumed in equilibrium with the organic inputs from vegetation) can be sampled from the field and then incubated without further amendments (Wadman and deHaan, 1997). A change in land use resulting in a sudden change in input (e.g., long-term bare fallow experiments) could also be employed to assess decomposition rates by tracking the temporal changes of SOM after the disturbance (Barré et al., 2010; Kuzyakov, 2011). Alternatively, isotope dilution can be used to track changes in C after such transitions as between C3 and C4 vegetation (Bernoux et al., 1998; Derrien and Amelung, 2011; Kuzyakov, 2011). In all these cases the decomposed sample contains materials of different ages, or multiple cohorts, so that the solutions derived for a single input or one cohort of uniform age are invalid. To model these experiments, we assume an instantaneous change in the otherwise continuous litter input to the soil (Fig. 1B). This change can be used to estimate decomposition parameters, similarly to litterbag studies. In this case, however, SOM or mixed litter samples contain a mixture of compounds that are the result of the previous history of input and degradation.

As illustrated in Fig. 1B, these experiments are modeled by a step change in input $I(t)$ at time $t = 0$, from I_1 to I_2. In the particular case of laboratory incubations or long-term bare fallow studies, $I_2 = 0$ and $t = 0$ is the time of sampling. For simplicity, we also assume that before sampling or disturbance, the soil had reached an equilibrium point under input I_1, denoted as x_1^* (i.e., the initial mass for the decomposition experiment), and that the change in chemical composition of the litterfall is less important than the actual input change. To find the mass remaining, we first separate the integral in Eq. (1) into two time intervals, corresponding to input I_1 before the sampling time, and to I_2 afterwards,

$$x(t) = \int_t^\infty I_1 A(\tau)d\tau + \int_0^t I_2 A(\tau)d\tau \tag{5}$$

Recalling that the mean transit time $\bar{\tau} = \int_0^\infty A(\tau)d\tau$, and that the steady state organic matter contents are $x_1^* = \bar{\tau}\cdot I_1$ and $x_2^* = \bar{\tau}\cdot I_2$ (as easily shown by imposing a constant input in Eq. (1)), Eq. (5) can be re-written as,

$$x(t) = x_1^* - (I_1 - I_2)\int_0^t A(\tau)d\tau \tag{6}$$

At $t = 0$, the integral on the right hand side is zero, so that we are left with the C mass before the experiment starts, $x(t) = x_1^*$. At later times, $\int_0^t A(\tau)d\tau$ approaches the mean transit time $\bar{\tau}$, so that $x(t)$ nears x_2^*, the steady state organic matter resulting from the input I_2 after the step change. This result is expected, as the system changes from a state dependent on I_1 to a new state dependent on I_2. At intermediate time periods, because the survivor function and its integral are by definition positive, the remaining mass $x(t)$ decreases through time if $I_1 - I_2 > 0$, or increases if $I_1 - I_2 < 0$.

For most practical applications, including SOM incubations and isotope dilution approaches, $I_2 = 0$, so that the fraction of mass remaining can be expressed as

$$\frac{x(t)}{x^*} = 1 - \frac{1}{\bar{\tau}}\int_0^t A(\tau)d\tau, \tag{7}$$

where the subscript 1 is dropped for simplicity of notation. Note that Eq. (7) has the same physical meaning as Eq. (2) (describing how C mass relative to the initial condition changes over time), but it is formally different due to the presence of old material in SOM samples.

As for the single input case, we can compute the apparent decay rate from the lumped mass balance,

$$\frac{dx(t)}{dt} = -k_{app}^*(t)x(t), \tag{8}$$

with initial condition $x(0) = x^*$. After some rearrangement and using again the definition of mean transit time, the apparent decay rate for multiple-cohort studies is obtained,

$$k_{app}^*(t) = \frac{A(t)}{\int_t^\infty A(\tau)d\tau} \tag{9}$$

Despite Eq. (9) being analogous to Eq. (4) obtained for single cohorts, it is mathematically different because the model now accounts for the presence of old C in the decomposing material. The obtained $x(t)$ and $k_{app}^*(t)$ for each model are reported in Table A2.

2.3. Description of the decomposition models

The equations for mass loss and apparent decay rate depend on the survivor function $A(t)$, which accounts for the different model structures. In this section we review the features of the eight selected models (Table 1), while the different $A(t)$ are reported in Table A1. Because decomposition time series typically consist of few measurement points for any substrate and location, it is important to minimize the number of model parameters. This justifies the use of simple models with at most three parameters for our analysis (Table 1). Using complex models with more variables, and thus more parameters, would likely lead to over-fitting issues for the type of dataset used here (Section 2.4). This would result in multiple, practically undistinguishable, solutions obtained from different sets of parameters for the same model, or also from different models because of poor constraining by the data.

We present only a brief overview of the models here, because they have already been studied and described extensively (Andren and Katterer, 1997; Thuries et al., 2001; Bruun et al., 2004; Pansu et al., 2004; Manzoni et al., 2009; Derrien and Amelung, 2011). The discrete compartment models (D1 to D4 in Table 1) are characterized by a network of C pools connected by first-order fluxes. Model D1 considers a single well-mixed compartment for all organic matter and is the simplest representation of the decomposition process. The serial model D2 mimics the sequential transformations of organic matter, where a fraction r of the C from the first compartment is lost to respiration and leaching, while the remaining fraction 1-r is transferred to the second C pool. In the parallel model D3, added organic matter is partitioned into two chemically different pools according to the coefficient α. From these pools, C is decomposed according to two different decay rates. The feedback model D4 accounts for microbial degradation and recycling of organic substrates in the first pool. The fraction r of the decomposed C is respired (or leached), while the fraction 1-r is used for growth of new biomass in the microbial pool (i.e., 1-r is the microbial C-use efficiency). Microbial byproducts are eventually returned to the substrate pool. All of these discrete compartment models can be recast in the form $dx(t)/dt = I(t) - k_{app}(t)x(t)$, where $k_{app}(t)$ depends on the particular history of litter input, as shown by Eqs. (4) and (9).

Notably, the survivor function of models D2–D4 can be expressed as the sum of two exponential terms with distinct decay rates (equivalent to $A(t)$ from model D3, see Table A1). Hence, when

fitting a set of decomposition data, the two-pool models yield the same least-square solution $x(t)$ (from Eq. (2) or (7)), where, however, the physical meaning of the parameters varies among models. By comparing $A(t)$ of models D2 and D3, we can write the parameters of D2 (superscript *D2*) as a function of the parameters in D3 (superscript *D3*),

$$\begin{aligned} k_1^{D2} &= k_1^{D3}, \\ k_2^{D2} &= k_2^{D3}, \\ r^{D2} &= 1-(1-\alpha)\left(k_1^{D3}-k_2^{D3}\right)\Big/k_1^{D3}. \end{aligned} \tag{10}$$

Comparing models D4 and D3, we can similarly express the parameters of D4 (superscript *D4*) as a function of those in D3,

$$\begin{aligned} k_1^{D4} &= \frac{\alpha k_1^{D3^2}+(1-\alpha)k_2^{D3^2}}{\alpha k_1^{D3}+(1-\alpha)k_2^{D3}}, \\ k_2^{D4} &= \left(\frac{\alpha}{k_2^{D3}}+\frac{1-\alpha}{k_1^{D3}}\right)^{-1}, \\ r^{D4} &= \frac{\left[\alpha k_1^{D3}+(1-\alpha)k_2^{D3}\right]^2}{\alpha k_1^{D3^2}+(1-\alpha)k_2^{D3^2}}. \end{aligned} \tag{11}$$

These relationships allows us to perform one least-square fitting for model D3 (the simplest mathematically) and compute the parameters for the other two-pool models analytically.

Instead of defining a set of compartments and deriving $k_{app}(t)$ as in models D1–D4, it is also possible to define *a priori* a decay $k_{app}(t)$ that allows mathematically simple expressions to fit the decomposition data. Following this alternative approach, lumped models with time-dependent decay rates (L1 and L2 in Table 1) have been proposed (Janssen, 1984; Yang and Janssen, 2000; Feng and Li, 2001; Rovira and Rovira, 2010). In these models the decay rate of a single pool decreases over time following either a power-law (L1) or an exponential decay (L2). Not all $k_{app}(t)$ functions, however, are consistent with a finite mean transit time and hence with a finite organic matter mass at equilibrium – a necessary condition for Eq. (1) to be applicable.

Table 1 also includes two continuous-quality models (C1 and C2) that assume a distribution of decay rates in the organic matter sample (Tarutis, 1994; Bolker et al., 1998; Forney and Rothman, 2007). These can be regarded as generalizations of the discrete parallel model (D3), where the number of compartments is increased (while their size decreases) so to obtain a continuous sequence of infinitesimal pools, each decomposing independently according to first-order kinetics. The initial partitioning of the added organic matter is defined by the distribution $p_k(k)$, which in the two selected models is either a gamma (C1) or a log-uniform distribution (C2). For these continuous models, the survivor function is calculated as the exceedance probability of the transit time distribution, which in turn depends on $p_k(k)$ (Manzoni et al., 2009).

2.4. Application data and statistical analyses

To provide specific examples of the different equations, we selected two published long-term decomposition experiments. For the single cohort case, we selected a set of Scots pine (*Pinus sylvestris*) decomposition data conducted at Jädraås, Sweden (Berg et al., 1991). Litterbags in the study were filled with freshly senesced pine needles, placed on the ground, and sampled 2–3 times per year for a total incubation of 5.5 years, resulting in nearly 80% mass loss. For the multiple cohort (SOM) case, we chose the Rothamsted Bare Fallow experiment, started at Rothamsted Experimental Station (UK) in 1959, to track the decay of organic C in absence of any organic inputs to the soil (Barré et al., 2010). Total C concentrations have been routinely measured and corrected to account for changes in soil bulk density. Over about 50 years, nearly 65% of the initial C has been lost.

Data for the amount of mass remaining in both datasets have been fitted with the solutions presented in Tables A1 and A2 for the litter application and the soil organic C application, respectively, using a nonlinear least-square approach (Gauss–Newton method, implemented in Matlab, MathWorks, 2011). All data points have been equally weighted and no transformation was performed prior to the fitting (the variance remains relatively stable through time). Goodness of fit was evaluated using the coefficient of determination and the mean square error, while the performance relative to the number of model parameters was evaluated using the Akaike information criterion, AIC (Akaike, 1974), and the Bayesian information criterion, BIC (Schwarz, 1978). Both criteria balance goodness of fit and model complexity (an undesired source of variance) in a single metric. In most decomposition studies, the number of data points, N, is relatively small (<40 times the number of model parameters), so that the second-order variant of AIC is used (Burnham and Anderson, 2002; Adair et al., 2008; Rovira and Rovira, 2010). This variant is denoted by *AICc* and is defined for a model j as,

$$AICc_j = N\ln\left(\frac{RSS_j}{N}\right) + \frac{2Np_j}{N-p_j-1}, \tag{12}$$

where RSS_j is the residual sum of squares (used here to estimate the maximum likelihood function), and p_j the number of model parameters (including the estimated maximum likelihood function as an additional parameter). The BIC for model j is calculated using a somewhat similar expression, except for the effect of the number of observations (Schwarz, 1978),

$$BIC_j = N\ln\left(\frac{RSS_j}{N}\right) + p_j\ln(N). \tag{13}$$

As the number of fitting parameters increases, the residual sum of squares (and thus the first term in Eqs. (12) and (13)) decreases, while the second term increases in both metrics. The best model in term of balance between goodness of fit and parsimony is the one with lower $AICc_j$ or BIC_j. Because the values of both indices have relevance on a relative scale, we only report the differences $AICc_j - min\ (AICc)$ and $BIC_j - min\ (BIC)$ (Burnham and Anderson, 2002). As a consequence, the best model has AIC or BIC differences equal to zero. We also tested the robustness of the model selection by performing a bootstrap sampling and replacing (Efron, 1979), and analyzing the resulting probability of model selection. A Matlab code that performs the fitting to single- or multiple-cohort data and evaluates the goodness of fit of the different models is available upon request.

3. Results and discussion

3.1. Application to litterbag decomposition data (single cohort)

All of the analytical expressions in Table A1 are able to explain most of the variability in the observed mass remaining data (Fig. 2A–C; Table 2). The single-compartment model (D1) performs marginally worse than the other models, as expected from the presence of only one fitting parameter instead of two or three. The discrepancy is evident only in the later stages of decomposition, where D1 underestimates remaining mass considerably. In contrast, all other models capture both the initial fast decay and the later slower mass loss. Series, parallel, and feedback models (D2–D4) predict the same decomposition pattern, because they can all be recast in the same analytical function, despite having

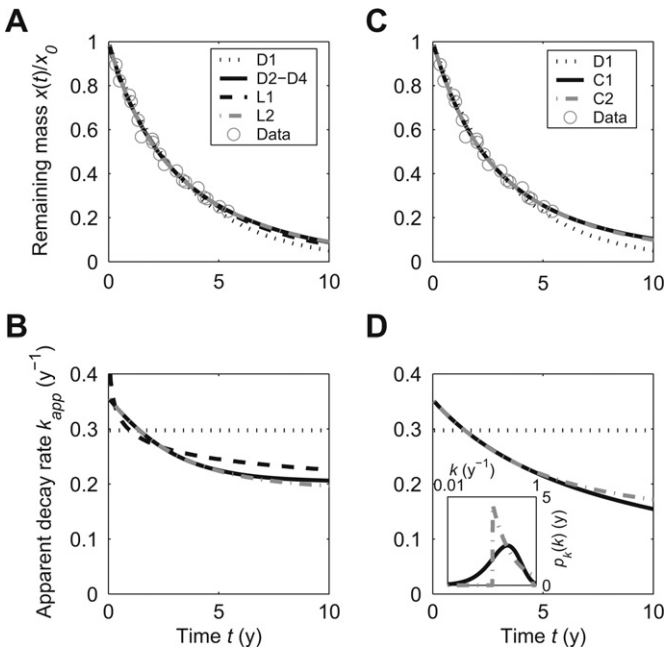

Fig. 2. Mass remaining, $x\,(t)/x_0$, and apparent decay rates, $k_{app}(t)$, as a function of time calculated for litter decomposition data (Berg et al., 1991) with discrete compartment and lumped, time-dependent rate models (A–B) and with continuous quality models (C–D) (results for the single pool model, D1, are also shown for comparison). Note that the curves for the two-pool models D2, D3, and D4 are identical; the inset in D shows the distribution of decay rates $p_k(k)$ for the two continuous quality models (C1 and C2). Models are described in Table 1 and equations are reported in Table A1.

a different structure in terms of the C pathways. Overall, the continuous quality models (C1 and C2) predict larger fractions of remaining mass after about 5 years since the beginning of the experiment. When balancing goodness of fit and parsimony, both of these models perform better than the discrete ones and should be preferred according to AIC and BIC (the result is robust to variability in the data as analyzed by bootstrapping, with 67% cases best described by C2, 12% by C1, and most of the remaining cases by L1). Moreover, C1 predicts a power-law decay of remaining mass in time (Table A1), similar to the solution obtained using specific parameterizations of the Q-model, a more general continuous-quality model (Bosatta and Ågren, 1995; Ågren and Bosatta, 1996). Power-law decay, especially when parameter a is close to or lower than 1, is characterized by relatively large remaining C in the long-term. Model C1 might thus be suitable to describe the very slow decay rates of compartments representing recalcitrant organic matter without the disadvantage of a complex parameterization of the slower pools. Overall, AIC and BIC differences are relatively low and model performance is high (except for D1), suggesting that, despite a marginally better performance of the continuous models, this dataset does not allow selecting a single 'best' model. A larger number of data points, especially towards the later stages of decomposition, would probably better constrain the models and provide a more definite indication.

A time-dependent apparent decay rate naturally arises when the underlying model has more than one compartment, even with all fluxes described by constant kinetic rates (Fig. 2B–D). As expected, the apparent decay rate decreases in time in all models except D1, which assumes a constant decay rate for a C pool that is perfectly well-mixed. In fact, $k_{app}(t)$ accounts for the changes in relative weights of the pools as they decompose. During initial decomposition, most of the mass loss is attributable to fast-decaying pools, so that $k_{app}\,(t)$ is high. As decomposition progresses, however, these fast pools lose mass, while the slower ones become the predominant contributors, resulting in lower $k_{app}(t)$. When $k_{app}(t)$ decreases too rapidly to zero, a residual mass may remain undecomposed (e.g., $a < 1$ in C1). In this case, in the presence of a continuous input the system cannot reach equilibrium, but instead C accumulates (as in peatlands under anaerobic condition). This lack of steady state implies that the equations developed in Section 2 for multiple cohorts cannot be used, as noted by Feng (2009a).

Although the mass remaining functions produced similar estimates between models (Fig. 2A–C), the changes in k_{app} over time differed between them (Fig. 2B–D). In the two-pool models, $k_{app}(t)$ tends to a constant value (the decay rate of the slower pool, k_2) when $t >> 1/k_1$, i.e., when the faster pool has been depleted. Consistent with higher remaining mass for large t, $k_{app}(t)$ in the C1 and C2 models are lower than in the other models. However, while $k_{app}(t)$ in L2 and C2 reaches stable values, $k_{app}(t)$ in L1 and C1 decreases indefinitely following a power-law behavior (as can be shown by taking $t \to \infty$ in $k_{app}(t)$ from Table A1). Because the models were adjusted to a single-cohort litter study, these decreases in k_{app} should be associated with the chemical composition of the litter rather than to possible differences in the ages of the litter material, as suggested for SOM studies in the next section.

Model parameters in C1 and C2 also determine the shape of the distribution of initial decay rates, $p_k(k)$, in the incubated substrate. Based on the regression, it is thus possible to draw the corresponding distribution $p_k(k)$ (see inset in Fig. 2D). The two distributions overlap in the range of turnover times ($1/k$) between ~1 and 10 years, but the mode of $p_k(k)$ for C2 is lower (~0.1 y^{-1}) than the one for C1 (~0.25 y^{-1}). This difference is due to the limited range of decay rates that $p_k(k)$ spans in C2 ($a \le k \le b$), which causes a higher probability density of decay rates close to the minimum value $k = a$.

3.2. Application to SOM decomposition data (multiple cohort)

Decomposition of SOM (as multiple cohort litter samples) containing C compounds deposited to the soil at different times tends to be slower than in homogenous fresh litter samples (compare the mean transit times in Tables 2 and 3). Slower decomposition is expected as recalcitrant compounds encompass a larger fraction of the total organic matter (Berg and McClaugherty, 2003). The widely-used, single-compartment model D1 assumes that the

Table 2
Summary of parameter values, mean transit times $\bar{\tau}$, and model performance statistics (coefficient of determination R^2, mean square error, RSS_j/N, as well as *AICc* and *BIC* differences) from fitting litter decomposition data (Fig. 2).

Model	Parameter values	$\bar{\tau}$ (y)	R^2	RSS_j/N	$AICc_j - min\,(AICc)$	$BIC_j - min\,(BIC)$
D1	$k = 0.297\ y^{-1}$	3.4	0.98	7.04E-04	13.2	12.9
D2	$r = 0.529$, $k_1 = 0.672\ y^{-1}$, $k_2 = 0.204\ y^{-1}$	3.8	0.99	2.92E-04	2.8	2.8
D3	$\alpha = 0.324$, $k_1 = 0.672\ y^{-1}$, $k_2 = 0.204\ y^{-1}$	3.8	0.99	2.92E-04	2.8	2.8
D4	$r = 0.725$, $k_1 = 0.491\ y^{-1}$, $k_2 = 0.385\ y^{-1}$	3.8	0.99	2.92E-04	2.8	2.8
L1	$a = 0.882$, $b = 3.447$ y	3.7	0.99	3.19E-04	1.5	1.5
L2	$a = 0.190\ y^{-1}$, $b = 0.167\ y^{-1}$, $m = 0.321\ y^{-1}$	3.8	0.99	2.93E-04	2.8	2.9
C1	$a = 2.746$, $b = 7.783$ y	4.5	0.99	2.94E-04	0.0	0.0
C2	$a = 0.103\ y^{-1}$, $b = 0.842\ y^{-1}$	4.0	0.99	2.93E-04	0.0	0.0

Table 3
Summary of parameter values, mean transit times $\bar{\tau}$, and model performance statistics (coefficient of determination R^2, mean square error, RSS_j/N, as well as *AICc* and *BIC* differences) from fitting of SOM decomposition data (Fig. 3).

Model	Parameter values	$\bar{\tau}$ (y)	R^2	RSS_j/N	$AICc_j - min\ (AICc)$	$BIC_j - min\ (BIC)$
D1	$k = 0.0231\ y^{-1}$	43.2	0.68	6.39E-03	47.3	46.2
D2	$r = 0.870$, $k_1 = 0.221\ y^{-1}$, $k_2 = 0.0125\ y^{-1}$	14.8	0.96	7.23E-04	0.0	0.2
D3	$\alpha = 0.863$, $k_1 = 0.221\ y^{-1}$, $k_2 = 0.0125\ y^{-1}$	14.8	0.96	7.23E-04	0.0	0.2
D4	$r = 0.879$, $k_1 = 0.220\ y^{-1}$, $k_2 = 0.0143\ y^{-1}$	14.8	0.96	7.23E-04	0.0	0.2
L1	$a = 0.236$, $b = 0.0940$ y	3.2	0.96	8.17E-04	0.3	0.0
C1	$a = 1.415$, $b = 6.727$ y	16.2	0.95	9.15E-04	3.1	2.7
C2	$a = 0.00906\ y^{-1}$, $b = 20.42\ y^{-1}$	14.3	0.88	2.28E-03	25.0	24.7

organic matter is perfectly mixed, and hence each particle has equal probability of being degraded at any time. Accordingly, this is the only model that does not capture the different decomposability of fresh *vs.* old organic matter. The decay of SOM is shown in Fig. 3, which compares the trajectories of remaining mass (3A–C) and the apparent decay rates (3B–D) for all models except L2, which is not amenable to an analytical solution for multiple cohorts. Similar to the single-cohort result, the performance of D1 is worse than in the other models and the simplicity of this one-parameter model does not justify its use according to AIC and BIC (Table 3). The well-mixed model severely overestimates mass remaining in the early decomposition stage and underestimates it in the later stage. Unlike the single-cohort case, however, the discrete models D2–D4 tend to outperform the other models in terms of both accuracy and parsimony (based on the bootstrap analysis, about 86% and 78% of datasets are best described by the two-pool models according to AIC and BIC, respectively). However, the improvement over model L1 (selected in 11% and 19% of the datasets according to AIC and BIC) is barely detectable (Table 3). As in the single-cohort case, model performance is generally good in all models except for D1 and C2.

Decomposition of single and multiple cohorts can be compared by plotting mass remaining and apparent decay rates for the two cases using the same parameters obtained from a single cohort incubation (Fig. 4). These simulations represent changes of $x(t)$ through time observed in a hypothetical experiment providing mass remaining in both a single cohort of litter and a litter mixture of the same origin, assuming that the mixture had reached the steady state before the experiment. As expected, remaining mass in incubations of multiple litter cohorts, denoted by $x(t)/x^*$, is always higher than in the case of a single cohort litter, denoted by $x(t)/x_0$, while the apparent decay rate is lower in multiple cohorts than in single cohort incubations ($k^*_{app}(t) < k_{app}(t)$) except for model D1, where k_{app} is always constant and equal in both experiments. The differences between the trajectories in the two experiment types are larger at intermediate times for all models. In fact, for both experiments the trajectories are controlled by the slower compartments, so that in the long term, $x(t)/x_0 \approx x(t)/x^*$. Accordingly, both $k_{app}(t)$ and $k^*_{app}(t)$ for models D2-D4 approach the value of the slower pool, k_2, as the faster pool is depleted (Fig. 4B). Patterns of $k^*_{app}(t)$ are more diverse

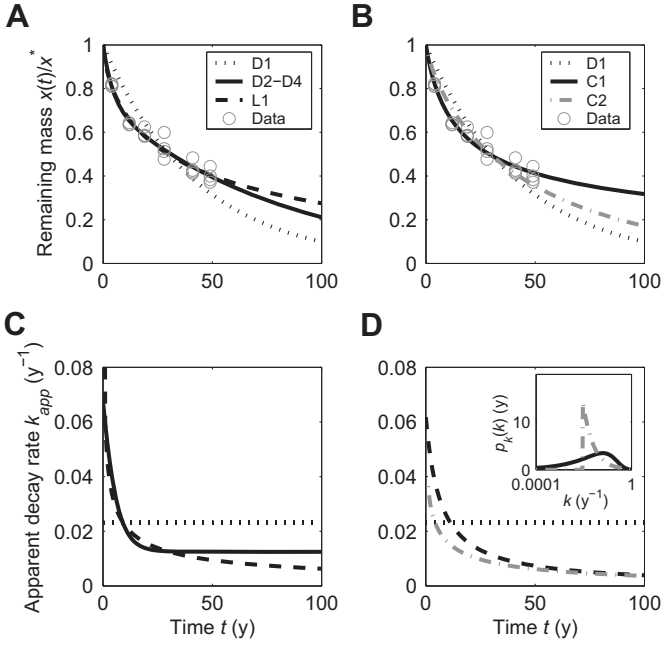

Fig. 3. Mass remaining, $x(t)/x^*$, and apparent decay rates, $k^*_{app}(t)$, as a function of time calculated for soil organic matter decomposition data (Barré et al., 2010) with discrete compartment and lumped, time-dependent rate models (A–B) and with continuous quality models (C–D) (results for the single pool model, D1, are also shown for comparison). Note that the curves for the two-pool models D2, D3, and D4 are identical; the inset in D shows the distribution of decay rates $p_k(k)$ for the two continuous quality models (C1 and C2). Models are described in Table 1 and equations are reported in Table A2.

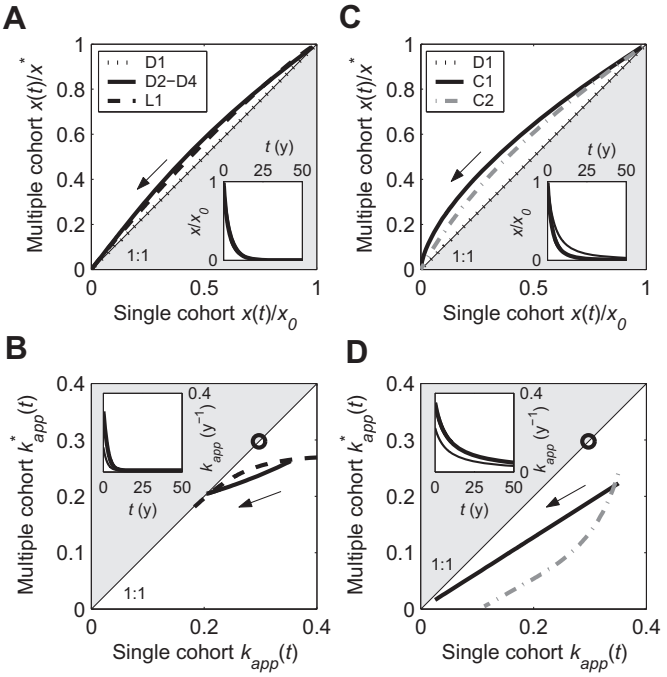

Fig. 4. Comparison of mass remaining (panels A, C) and apparent decay rates (panels B, D) estimated for the same set of parameters (Table 2) for single- *vs.* multiple-cohort equations, as they change over time following the arrows. Temporal changes are also shown as examples for models D3 and C1 in the insets, where changes of mass remaining and k_{app} for the single- (thick line) and multiple cohort (thin line) equations are illustrated. The 1:1 line represents the case where the estimates for the two cases are equal and the shaded areas indicate where decomposition is faster in the multiple-cohort samples than in the single cohort ones – an unrealistic condition since decomposition will be always faster in single cohorts (see Section 3.3). Panels A and B show results for discrete compartment and lumped, time-dependent rate models and panels C and D for continuous quality models. In panels B and D, open circles on the 1:1 line represent the apparent decay rates for the single-pool model, for which the single- and multiple-cohort equations are equal.

among lumped and continuous quality models, with $k^*_{app}(t)$ reaching an asymptotic value in L1 and C2, but tending towards zero in C1. The mathematical relationship between $k^*_{app}(t)$ and $k_{app}(t)$ is particularly clear in C1, where $k^*_{app}(t) = k_{app}(t)(a-1)/a$, i.e., the two apparent decay rates differ by a constant that only depends on parameter a (Fig. 4D).

3.3. Model interpretation

The models presented in Table 1 can be interpreted from a biophysical perspective, thus providing natural bounds for the parameter values. The decay rates of the different compartments in D1–D4 characterize their chemical and physical properties, and are expected to vary with climate (Berg and McClaugherty, 2003; Parton et al., 2007; Zhang et al., 2008), soil texture (Parton et al., 1987), and litter quality (Aerts, 1997; Cebrian, 1999; Berg and McClaugherty, 2003; Cornwell et al., 2008; Hui and Jackson, 2009). The values of the kinetic constants in D1–D4 (k, k_1, and k_2) from the litter application are higher than in the SOM application (Tables 2 and 3). This difference is due to several factors, namely the different qualities of the plant material and climatic conditions, as well as to the 'protecting' effect of mineral soil that prevents SOM degradation (Sollins et al., 1996; Kleber et al., 2007). The latter is likely the most relevant factor for a given site, and might contribute to the stark contrast between the kinetic constants of the slow C pools in litter and SOM. In fact, while the fast pools differ by a factor of two between litter and SOM studies, the slower ones differ by an order of magnitude in all models (Tables 2 and 3).

The coefficient r in D2 and D4 can be interpreted as the fraction of decomposed matter that is lost to respiration by the decomposers (1-r is the C-use efficiency) or by leaching. Indeed, the estimated values for litter decomposition (Table 2) are consistent with C-use efficiency estimates 1-r ~ 0.3 to 0.4 for conifer litter decomposers (Manzoni et al., 2010). Respiration rates estimated from SOM decomposition (Table 3) are higher, suggesting lower C-use efficiency in this soil. Because typically in mineral soils $r \sim 0.4$–0.6 (Frey et al., 2001; Steinweg et al., 2008; Herron et al., 2009), we might speculate that the parameter r also captures leaching losses from the faster C compartments, which are expected to be important in the mesic climate of Rothamsted, especially in absence of vegetation in this long-term fallow treatment. Because the selected decomposition data do not allow distinguishing among the two-pool models, other types of experiments are needed to contrast the performance of parallel, series, and feedback configurations. For example, labeling experiments tracking the fate of C isotopes in different pools (and fluxes) might be useful to this aim (Petersen et al., 2005).

The parameters in models L1 and L2 are more difficult to interpret, as they were designed to represent in a lumped way the observed rates of mass decay, rather than to describe them in a process-based way. The two continuous-quality models we considered (C1 and C2) can be interpreted as a generalization of the discrete-compartment models, where now the decay rates follow a continuous distribution caused by heterogeneous quality and accessibility of the substrates (Tarutis, 1994; Ågren and Bosatta, 1996; Rothman and Forney, 2007; Bruun et al., 2010). Our results suggest that litter can be indeed characterized by a distribution of decay rates that represents a range of transit times (or life spans) of C molecules in a litter cohort. In contrast to this continuous range of transit times, the SOM decomposition dataset we analyzed is characterized by two distinct time scales (a fast and a slow pool, see e.g., Taneva et al., 2006) that can be captured well by two-pool models, but not as well by continuous models based on a unimodal distribution of k, as in C1 and C2. The goal of the data analysis here was to provide an example of application of the theoretical equations, but it is too limited to generalize this conclusion to any soil or litter. Further studies across litter and soil types and of both SOM and litter decomposition at same locations will be needed to accomplish this goal.

Each model permits the definition of the organic carbon mean transit time $\bar{\tau}$ (or the time that on average a molecule of C spends in the system – in general different from the turnover time), which is derived from estimated model parameters (see equations in Table 1) (Manzoni et al., 2009). Despite fitting the same datasets, the models provide different estimates of $\bar{\tau}$, due to their different compartment structure. This is particularly true for the SOM data, where the well-mixed model D1 yields a transit time about three times higher than the better-performing two-compartment models. Thus, in this case, the well-mixed model significantly overestimates $\bar{\tau}$, as also found in previous studies (Taneva et al., 2006). In contrast, model L1 provides a much shorter estimate, due to its very fast initial decomposition (see the dashed line in Fig. 3C). These differences highlight the importance of model choice when estimating mean transit times (Derrien and Amelung, 2011) as well as steady state C stocks ($x^* = \bar{\tau} \cdot I$).

The mean transit time provides only limited information regarding the temporal changes in C turnover. One way to explore such changes is by looking at the apparent decay rates $k_{app}(t)$, that is, the time-dependent kinetic constant representing the relative change in organic matter, $-(dx/dt)/x$ (Eqs. (3) and (8)). Empirical observations suggest that k_{app} decreases over time (Wieder and Lang, 1982; Janssen, 1984; Yang and Janssen, 2000; Rovira and Rovira, 2010). This decrease is due to the exhaustion of fast-cycling pools (with high k) early during decomposition, followed by prolonged respiration from the slower pools (low k). The analytical results reported in Tables A1 and A2 for all models except D1 are consistent with this pattern. Only the well-mixed model is characterized by a constant k_{app}, thus underestimating the early decay rates, while overestimating decomposition in the later stages (Trumbore, 2000). Even for the same set of parameters (i.e., the same chemical characteristics), k_{app} is lower in multiple-cohort studies than in single cohort ones (Fig. 4B–D). This is due to the presence of older (and slower) cohorts that decrease the apparent decay rate in the multiple cohort studies. Using the two sets of equations for single or multiple cohort studies, it is thus possible to separate the chemical from the age-related effects on mass loss and k_{app}.

3.4. Disentangling causes of variation in decomposition patterns

The proposed theory allows us to separate the causes of mass loss and the decrease in k_{app} over time. At a given site, there are three sets of drivers for such temporal changes, i) initial chemical composition, ii) age distribution in the sample, and iii) differences in the abiotic environment (e.g., different temperature, soil moisture, and mineral particles between mineral soil and forest floor). In surface litter, only i) and ii) play a role. If we further look at a particular litter type (and chemical composition), the age distribution at the beginning of decomposition, determined by the previous input history, becomes the most important factor. In this case, the decay constants of each C pool should be the same in single- and multiple-cohort litter samples, because only the input history differs between the two cases, and multiple cohorts are collections of inputs of the same litter over time. The overall decomposition rate (as well as k_{app}), however, are lower for multiple-cohort samples because relatively more material with slow turnover is present. These different dynamics of single and multiple cohorts (even with the same kinetic constants) are captured by Eq. (1) when assuming different input histories (Tables A1 and A2). Fig. 4 compares these two cases by showing the remaining mass in a single cohort against the remaining mass for multiple cohorts, assuming the parameters of the models are the

same. In this example, the differences of the trajectories from the 1:1 line are entirely due to different initial age distribution in the sample.

In principle, the mass decay equations calibrated for a single litter cohort could be used to predict decomposition of the surface litter pool composed of multiple litter cohorts (Fig. 4). However, litter decay rates cannot be used for SOM, because bio-physical mechanisms controlling decomposition in soils are different from surface litter (factor iii in the list above), so that the model parameters (if not the model structure itself) are expected to change. One way to quantify these changes due to the specific soil environment is to compare predicted mass loss for multiple litter cohorts to measured SOM mass loss from the same site. In this way the three factors outlined above can be effectively disentangled. Considering one litter type, chemical differences in the original material are avoided, whereas age-related effects in multiple litter cohorts can be captured by the equations in Table A2 with parameter values obtained from a single cohort decomposition study (Table A1). Finally, the role of abiotic factors in the soil can be quantified by comparing simulations for multiple litter cohorts to measured SOM mass loss data. New studies examining simultaneously single and multiple litter cohorts as well as SOM decomposition at a specific location would help distinguish the effects of these different controls on decomposition.

3.5. Conclusions

We systematically examined different decomposition models to describe mass remaining and apparent decay rates for two types of experiments: i) single cohort (e.g., litterbag), and ii) multiple cohort (SOM) decomposition studies, obtaining for both types analytical equations that can be used to fit decomposition data across substrate types and climatic conditions. The equations derived for SOM data are different from the ones for single cohorts, implying that care should be taken when selecting a mathematical equation to fit the decomposition data. The model inter-comparison showed that the often used, single-compartment exponential model performs poorly with respect to two-compartment models, lumped models with time-dependent kinetic rates, and continuous quality models. The increase in complexity of the two- and three-parameter models is statistically justified considering their increased accuracy. In an example from a litterbag decomposition study, the continuous quality models had the best balance between accuracy and model parsimony. In contrast, a dataset of long-term SOM decomposition data was best described by two-pool models, possibly because of the strong separation of time scales in this particular example. However, differences in model performance were too small to be able to select a single 'best' model for these datasets. All models (except the single-compartment one) predict that the apparent decomposition rate ($k_{app} = -(dx/dt)/x$) decreases over time. The parameters obtained from the model fitting can be physically interpreted to investigate decomposition patterns and model performance across climatic, vegetation, and edaphic conditions. Moreover, the proposed theoretical framework allows disentangling the different drivers of litter and SOM dynamics, thus permitting to clarify whether the observed mass loss patterns in different experiments (single *vs.* multiple cohorts; litter *vs.* SOM) are due to chemical differences in the original material, abiotic factors, or different age distributions in the sample. Applying the proposed equations to large datasets also including estimates for microbial biomass or other physically-based pools might provide indications for the most appropriate model structure to describe the decomposition process.

Acknowledgments

This research was supported by the United States Department of Energy (through the Office of Biological and Environmental Research, Terrestrial Ecosystem Science program, grant DE-SC0006967), the United States Department of Agriculture (USDA grant 2011-67003-30222), and the National Science Foundation (CBET-10-33467, DEB 0717191 and grant GEO-0452325 through the Inter-American Institute for Global Change Research, CRN II 2031). G. P. acknowledges the litter and SOM discussion group at IFEVA that contributed to some of the ideas presented in the paper, and was partially funded by PICT 2199, PIP 132, and UBACyT.

Appendix A

Relative mass loss $x(t)/x_0$ and apparent decay rates $k_{app}(t)$ for all selected models and for single- and multiple-cohort studies are reported in Tables A1 and A2. Note that the single-cohort relative mass loss is analytically equivalent to the survivor function, $x(t)/x_0 = A(t)$ (Eq. (2)).

Table A1
Analytical solutions for remaining mass after a single addition of litter, one cohort sample (e.g., litterbag incubations, $I = \delta(t)$).

Model	$x(t)/x_0 = A(t)$ (Eq. (2))	$k_{app}(t)$ (Eq. (4))
D1	e^{-kt}	k
D2	$\frac{(1-r)k_1e^{-k_2t} - (k_2-k_1r)e^{-k_1t}}{k_1-k_2}$	$k_1\frac{(1-r)k_2e^{k_1t} - (k_2-k_1r)e^{k_2t}}{(1-r)k_1e^{k_1t} - (k_2-k_1r)e^{k_2t}}$
D3	$\alpha e^{-k_1t} + (1-\alpha)e^{-k_2t}$	$\frac{\alpha k_1e^{-k_1t} + (1-\alpha)k_2e^{-k_2t}}{\alpha e^{-k_1t} + (1-\alpha)e^{-k_2t}}$
D4[a]	$\frac{\beta(1+e^{\beta t}) + (e^{\beta t}-1)(k_1(1-2r)+k_2)}{2\beta}e^{-\frac{(\beta+k_1+k_2)}{2}t}$	$\frac{k_1r[(e^{\beta t}-1)(k_1-k_2) - \beta(1+e^{\beta t})]}{(1-e^{\beta t})[k_2+k_1(1-2r)] - \beta(1+e^{\beta t})}$
L1	$e^{-\left(\frac{t}{b}\right)^a}$	$\frac{a}{b}\left(\frac{t}{b}\right)^{a-1}$
L2	$e^{-\frac{b}{m}(1-e^{-mt})-at}$	$a + be^{-mt}$
C1	$\frac{b^a}{(b+t)^a}$	$\frac{a}{b+t}$
C2[b]	$\frac{E_i(-bt) - E_i(-at)}{\ln(b/a)}$	$\frac{e^{-at}-e^{-bt}}{t[E_i(-bt) - E_i(-at)]}$

[a] For conciseness, we define $\beta = \sqrt{(k_1+k_2)^2 - 4k_1k_2r}$.

[b] $E_i(z)$: exponential integral, defined as $E_i(z) = -\int_{-z}^{\infty} e^{-u}/u\,du$ (Weisstein, 2011).

Table A2
Analytical solutions for the mass remaining in a multiple cohort sample such as soil organic matter (e.g., soil incubations, $I_1 > 0$, $I_2 = 0$).

Model	$x(t)/x^*$ (Eq. (7))[c]	$k^*_{app}(t)$ (Eq. (9))
D1	e^{-kt}	k
D2	$\frac{(1-r)k_1^2 e^{-k_2 t} - (k_2 - rk_1)k_2 e^{-k_1 t}}{(k_1 - k_2)[k_2 + (1-r)k_1]}$	$\frac{k_1 k_2[(1-r)k_1 e^{-k_2 t} - (k_2 - rk_1)e^{-k_1 t}]}{(1-r)k_1^2 e^{-k_2 t} - (k_2 - rk_1)k_2 e^{-k_1 t}}$
D3	$\frac{\alpha k_2 e^{-k_1 t} + (1-\alpha)k_1 e^{-k_2 t}}{\alpha k_2 + (1-\alpha)k_1}$	$\frac{k_1 k_2[\alpha e^{-k_1 t} + (1-\alpha)e^{-k_2 t}]}{\alpha k_2 e^{-k_1 t} + (1-\alpha)k_1 e^{-k_2 t}}$
D4[a]	$\left\{\frac{1+e^{\beta t}}{2} + \frac{(1-e^{\beta t})\gamma}{2\beta[(1-r)k_1 + k_2]}\right\} e^{-\frac{(\beta + k_1 + k_2)t}{2}}$	$\frac{k_1 k_2 r[\beta(1+e^{\beta t}) - (k_1 + k_2 - 2rk_1)(1-e^{\beta t})]}{\beta[(1-r)k_1 + k_2](1+e^{\beta t}) + \gamma(1-e^{\beta t})}$
L1[b]	$\frac{\Gamma\left[\frac{1}{a}, \left(\frac{t}{b}\right)^a\right]}{\Gamma\left[\frac{1}{a}\right]}$	$\frac{a e^{-\left(\frac{t}{b}\right)^a}}{b\Gamma\left[\frac{1}{a}, \left(\frac{t}{b}\right)^a\right]}$
C1	$b^{a-1}(b+t)^{1-a}, \quad a > 1$	$\frac{a-1}{b+t}$
C2	$\frac{be^{-at} - ae^{-bt} - [E_i(-bt) - E_i(-at)]abt}{b-a}$	$\frac{E_i(-bt) - E_i(-at)}{\frac{e^{-at}}{a} - \frac{e^{-bt}}{b} + [E_i(-bt) - E_i(-at)]t}$

[a] For conciseness, we define $\gamma = rk_1(k_1+3k_2)-(k_1+k_2)^2$.
[b] $\Gamma[\cdot, \cdot]$: incomplete gamma function (Abramowitz and Stegun, 1972).
[c] Model L2 is not included here as it does not allow an analytical solution for $x(t)/x^*$ in the general case $a > 0$ (for $a = 0$ no steady state can be reached).

References

Abramowitz, M., Stegun, I.A., 1972. Handbook of Mathematical Functions with Formulas, Graphs, and Mathematical Tables. U.S. Government Printing Office, Washington, DC.

Adair, E.C., Parton, W.J., Del Grosso, S.J., Silver, W.L., Harmon, M.E., Hall, S.A., Burke, I.C., Hart, S.C., 2008. Simple three-pool model accurately describes patterns of long-term litter decomposition in diverse climates. Global Change Biology 14, 2636–2660.

Aerts, R., 1997. Climate, leaf litter chemistry and leaf litter decomposition in terrestrial ecosystems: a triangular relationship. Oikos 79, 439–449.

Ågren, G.I., Bosatta, E., 1996. Theoretical Ecosystem Ecology. Understanding Element Cycles. Cambridge University Press, Cambridge, United Kingdom.

Akaike, H., 1974. New look at statistical-model identification. Ieee Transactions on Automatic Control AC 19, 716–723.

Andren, O., Katterer, T., 1997. ICBM: the introductory carbon balance model for exploration of soil carbon balances. Ecological Applications 7, 1226–1236.

Barré, P., Eglin, T., Christensen, B.T., Ciais, P., Houot, S., Katterer, T., van Oort, F., Peylin, P., Poulton, P.R., Romanenkov, V., Chenu, C., 2010. Quantifying and isolating stable soil organic carbon using long-term bare fallow experiments. Biogeosciences 7, 3839–3850.

Berg, B., McClaugherty, C.A., 2003. Plant Litter. Decomposition, Humus Formation, Carbon Sequestration. Springer.

Berg, B., Booltink, H., Breymeyer, A.I., Ewertsson, A., Gallardo, A.B.H., Johansson, M., Koivuoja, S., Meentemeyer, V., Nyman, P., Olofsson, J., Pettersson, A., Reurslag, A., Staaf, H., Staaf, I., Uba, L., 1991. Data on Needle Litter Decomposition and Soil Climate as Well as Site Characteristics for Some Coniferous Forest Sites. Part 2. Decomposition Data. Report 42. SwedishUniversity of Agricultural Sciences. Department of Ecology and Environmental Research, Uppsala, Sweden.

Bernoux, M., Cerri, C.C., Neill, C., de Moraes, J.F.L., 1998. The use of stable carbon isotopes for estimating soil organic matter turnover rates. Geoderma 82, 43–58.

Bolker, B.M., Pacala, S.W., Parton, W.J., 1998. Linear analysis of soil decomposition: insights from the century model. Ecological Applications 8, 425–439.

Bosatta, E., Ågren, G.I., 1995. The power and reactive continuum models as particular cases of the Q-theory of organic-matter dynamics. Geochimica Et Cosmochimica Acta 59, 3833–3835.

Bruun, S., Six, J., Jensen, L.S., 2004. Estimating vital statistics and age distributions of measurable soil organic carbon fractions based on their pathway of formation and radiocarbon content. Journal of Theoretical Biology 230, 241–250.

Bruun, S., Agren, G.I., Christensen, B.T., Jensen, L.S., 2010. Measuring and modeling continuous quality distributions of soil organic matter. Biogeosciences 7, 27–41.

Burnham, K.P., Anderson, D.R., 2002. Model Selection and Multimodel Inference. A Practical Information-Theoretic Approach, second ed. Springer.

Cebrian, J., Lartigue, J., 2004. Patterns of herbivory and decomposition in aquatic and terrestrial ecosystems. Ecological Monographs 74, 237–259.

Cebrian, J., 1999. Patterns in the fate of production in plant communities. American Naturalist 154, 449–468.

Cornwell, W.K., Cornelissen, J.H.C., Amatangelo, K., Dorrepaal, E., Eviner, V.T., Godoy, O., Hobbie, S.E., Hoorens, B., Kurokawa, H., Perez-Harguindeguy, N., Quested, H.M., Santiago, L.S., Wardle, D.A., Wright, I.J., Aerts, R., Allison, S.D., van Bodegom, P., Brovkin, V., Chatain, A., Callaghan, T.V., Diaz, S., Garnier, E., Gurvich, D.E., Kazakou, E., Klein, J.A., Read, J., Reich, P.B., Soudzilovskaia, N.A., Vaieretti, M.V., Westoby, M., 2008. Plant species traits are the predominant control on litter decomposition rates within biomes worldwide. Ecology Letters 11, 1065–1071.

Derrien, D., Amelung, W., 2011. Computing the mean residence time of soil carbon fractions using stable isotopes: impacts of the model framework. European Journal of Soil Science 62, 237–252.

Efron, B., 1979. 1977 Rietz Lecture – Bootstrap methods – Another look at the jackknife. Annals of Statistics 7, 1–26.

Eriksson, E., 1971. Compartment models and reservoir theory. Annual Review of Ecology and Systematics 2, 67–84.

Feng, Y.S., Li, X.M., 2001. An analytical model of soil organic carbon dynamics based on a simple "hockey stick" function. Soil Science 166, 431–440.

Feng, Y.S., 2009a. Fundamental considerations of soil organic carbon dynamics: a new theoretical framework. Soil Science 174, 467–481.

Feng, Y.S., 2009b. K-model-a continuous model of soil organic carbon dynamics: theory. Soil Science 174, 482–493.

Forney, D.C., Rothman, D.H., 2007. Decomposition of soil organic matter from physically derived decay rates. In: American Geophysical Union Fall Meeting. San Francisco, CA.

Frey, S.D., Gupta, V., Elliott, E.T., Paustian, K., 2001. Protozoan grazing affects estimates of carbon utilization efficiency of the soil microbial community. Soil Biology & Biochemistry 33, 1759–1768.

Herron, P.M., Stark, J.M., Holt, C., Hooker, T., Cardon, Z.G., 2009. Microbial growth efficiencies across a soil moisture gradient assessed using C-13-acetic acid vapor and N-15-ammonia gas. Soil Biology & Biochemistry 41, 1262–1269.

Hui, D.F., Jackson, R., 2009. Assessing interactive responses in litter decomposition in mixed species litter. Plant and Soil 314, 263–271.

Janssen, B.H., 1984. A simple method for calculating decomposition and accumulation of young soil organic-matter. Plant and Soil 76, 297–304.

Jenny, H., Gessel, S.P., Bingham, F.T., 1949. Comparative study of decomposition rates of organic matter in temperate and tropical regions. Soil Science 68, 419–432.

Jobbágy, E.G., Jackson, R.B., 2000. The vertical distribution of soil organic carbon and its relation to climate and vegetation. Ecological Applications 10, 423–436.

Kleber, M., Sollins, P., Sutton, R., 2007. A conceptual model of organo-mineral interactions in soils: self-assembly of organic molecular fragments into zonal structures on mineral surfaces. Biogeochemistry 85, 9–24.

Kuzyakov, Y., 2011. How to link soil C pools with CO_2 fluxes? Biogeosciences 8, 1523–1537.

Manzoni, S., Porporato, A., 2009. Soil carbon and nitrogen mineralization: theory and models across scales. Soil Biology & Biochemistry 41, 1355–1379.

Manzoni, S., Katul, G.G., Porporato, A., 2009. Analysis of soil carbon transit times and age distributions using network theories. Journal of Geophysical Research-Biogeosciences 114, G04025.

Manzoni, S., Trofymow, J.A., Jackson, R.B., Porporato, A., 2010. Stoichiometric controls dynamics on carbon, nitrogen, and phosphorus in decomposing litter. Ecological Monographs 80, 89–106.
MathWorks, T., 2011. Natick, MA.
Pansu, M., Bottner, P., Sarmiento, L., Metselaar, K., 2004. Comparison of five soil organic matter decomposition models using data from a C-14 and N-15 labeling field experiment. Global Biogeochemical Cycles 18, GB4022.
Parton, W.J., Schimel, D.S., Cole, C.V., Ojima, D.S., 1987. Analysis of factors controlling soil organic-matter levels in Great-Plains Grasslands. Soil Science Society of America Journal 51, 1173–1179.
Parton, W., Silver, W.L., Burke, I.C., Grassens, L., Harmon, M.E., Currie, W.S., King, J.Y., Adair, E.C., Brandt, L.A., Hart, S.C., Fasth, B., 2007. Global-scale similarities in nitrogen release patterns during long-term decomposition. Science 315, 361–364.
Petersen, B.M., Jensen, L.S., Hansen, S., Pedersen, A., Henriksen, T.M., Sorensen, P., Trinsoutrot-Gattin, I., Berntsen, J., 2005. CN-SIM: a model for the turnover of soil organic matter. II. Short-term carbon and nitrogen development. Soil Biology & Biochemistry 37, 375–393.
Plante, A.F., Parton, W., 2007. The dynamics of soil organic matter and nutrient cycling. In: Paul, E.A. (Ed.), Soil Microbiology, Ecology and Biochemistry. Elsevier, New York, NY, pp. 433–470.
Rothman, D.H., Forney, D.C., 2007. Physical model for the decay and preservation of marine organic carbon. Science 316, 1325–1328.
Rovira, P., Rovira, R., 2010. Fitting litter decomposition datasets to mathematical curves: towards a generalised exponential approach. Geoderma 155, 329–343.
Schwarz, G., 1978. Estimating Dimension of a model. Annals of Statistics 6, 461–464.
Sierra, C.A., Harmon, M.E., Perakis, S., 2011. Decomposition of heterogeneous organic matter and its long-term stabilization in soils. Ecological Monographs 81, 619–634.
Sollins, P., Homann, P., Caldwell, B.A., 1996. Stabilization and destabilization of soil organic matter: mechanisms and controls. Geoderma 74, 65–105.
Steinweg, J.M., Plante, A.F., Conant, R.T., Paul, E.A., Tanaka, D.L., 2008. Patterns of substrate utilization during long-term incubations at different temperatures. Soil Biology & Biochemistry 40, 2722–2728.
Taneva, L., Pippen, J.S., Schlesinger, W.H., Gonzalez-Meler, M.A., 2006. The turnover of carbon pools contributing to soil CO_2 and soil respiration in a temperate forest exposed to elevated CO_2 concentration. Global Change Biology 12, 983–994.
Tarutis, W.J., 1994. A mean-variance approach for describing organic-matter decomposition. Journal of Theoretical Biology 168, 13–18.
Thuries, L., Pansu, M., Feller, C., Herrmann, P., Remy, J.C., 2001. Kinetics of added organic matter decomposition in a Mediterranean sandy soil. Soil Biology & Biochemistry 33, 997–1010.
Trumbore, S., 2000. Age of soil organic matter and soil respiration: radiocarbon constraints on belowground C dynamics. Ecological Applications 10, 399–411.
Wadman, W.P., deHaan, S., 1997. Decomposition of organic matter from 36 soils in a long-term pot experiment. Plant and Soil 189, 289–301.
Weisstein, E.W., 2011. Exponential integral. In: MathWorld – A Wolfram Web Resource. http://mathworld.wolfram.com/ExponentialIntegral.html.
Wieder, R.K., Lang, G.E., 1982. A Critique of the analytical methods used in examining decomposition data obtained from litter bags. Ecology 63, 1636–1642.
Yang, H.S., Janssen, B.H., 2000. A mono-component model of carbon mineralization with a dynamic rate constant. European Journal of Soil Science 51, 517–529.
Zhang, C.F., Meng, F.R., Trofymow, J.A., Arp, P.A., 2007. Modeling mass and nitrogen remaining in litterbags for Canadian forest and climate conditions. Canadian Journal of Soil Science 87, 413–432.
Zhang, D., Hui, D., Luo, Y., Zhou, G., 2008. Rates of litter decomposition in terrestrial ecosystems: global patterns and controlling factors. Journal of Plant Ecology 1, 85–93.